

Characteristics of $\delta^{18}\text{O}$ in precipitation over Eastern Monsoon China and the water vapor sources

LIU JianRong^{1,2}, SONG XianFang^{1*}, YUAN GuoFu³, SUN XiaoMin³, LIU Xin^{1,2} & WANG ShiQin^{1,2}

¹Key Laboratory of Water Cycle & Related Land Surface Processes, Institute of Geographic Sciences and Natural Resources Research, Chinese Academy of Sciences, Beijing 100101, China;

²Graduate University of Chinese Academy of Sciences, Beijing 100049, China;

³CERN Sub-center of Water, Beijing 100101, China

Received December 16, 2008; accepted February 16, 2009; published online July 27, 2009

Monsoon circulation is an important carrier of water vapor transport, and it impacts the precipitation of the monsoonal regions through the constraints and controls of large-scale water vapor transport and distributions as well as the water vapor balance. An overall research on stable Hydrogen and Oxygen isotopes in precipitation over Eastern Monsoon China could benefit a comprehensive understanding of the monsoonal precipitation mechanism. Seventeen field stations of the Chinese Network of Isotopes in Precipitation (CHNIP) have been selected to collect monthly composite precipitation samples during the years 2005–2006. Components of δD and $\delta^{18}\text{O}$ have been analyzed to achieve the spatiotemporal distributions. The established Local Meteoric Water Line $\delta\text{D}=7.46\delta^{18}\text{O}+0.90$ based on the 274 obtained monthly samples could be treated as isotope input functions across the region, due to basically reflecting the specific regional meteorological conditions over Eastern Monsoon China. The δ -value depleted from coastal to inner area. In Southern China and Northeastern China there were typical periodic patterns of $\delta^{18}\text{O}$. Different dominant affecting meteorological factors have been raised with different regions. From south to north, the temperature effect of $\delta^{18}\text{O}$ enhanced, while the amount effect changed from existing at an all-year-scale in Southern China to being only remarkable during the main rainy seasons in North China and Northeastern China. Main geographical controls varied from altitude in Southern China and North China to latitude in Northeastern China. Furthermore, $\delta^{18}\text{O}$ had an implication of advance and retreat of the monsoon as well as rainfall belt transfer. $\delta^{18}\text{O}$ was also a tracer for the movement path of typhoon and tropical storms.

monsoon, precipitation, $\delta^{18}\text{O}$, Eastern Monsoon China (EMC), water vapour sources

Citation: Liu J R, Song X F, Yuan G F, et al. Characteristics of $\delta^{18}\text{O}$ in precipitation over Eastern Monsoon China and the water vapor sources. Chinese Sci Bull, 2010, 55: 200–211, doi: 10.1007/s11434-009-0202-7

The phenomenon of prevailing winds of large-scale areas change significantly with seasons is known as monsoon. The world's monsoonal regions are widely distributed, and China is located in the Asian Monsoonal Region [1]. Monsoon circulation is an important carrier of water vapor transport, and it impacts the precipitation of the monsoonal regions through the constraints and controls of large-scale water vapor transport and distributions as well as the water vapor balance [2–4]. Numerous studies have indicated that the environmental isotopes in precipitation have implica-

tions of tracing the water vapor sources and air mass transport pathway at different scales [5–12]. Sengupta et al. [13] pointed out that there were two main water vapor origins of precipitation in New Delhi during summer monsoonal period, and the rainfall proportions of the two origins have been calculated by using the isotopic fractionation models. Yamanaka et al. [14] obtained the water vapor sources of eastern Mongolia by analyzing the relationships between isotopes in precipitation and meteorological parameters. Pang et al. [4] determined the water vapor sources of New Delhi station, a representative of Southwestern Monsoonal Region, and Hong Kong station, a representative of South-

*Corresponding author (email: songxf@igsnr.ac.cn)

eastern Monsoonal Region. The results are generally in accordance with the basic atmospheric circulation background. Liu et al. [15] traced water vapor sources and transport pathways of Arid Northwestern China in different seasons using $\delta^{18}\text{O}$. It is obvious that the researches on stable isotopes in precipitation in Eastern Monsoon China being affected mostly by the monsoons are helpful to obtaining a comprehensive understanding of the monsoonal precipitation mechanism. Furthermore, a thorough study on precipitation isotopes is invaluable references for the interpretation of isotopic signal contained in the palaeoclimatic records. Original atmospheric signals (e.g. temperature and precipitation amount) could be reconstructed by a series of paleoarchives [16] such as ice cores [17], lacustrine sediments [18], tree-ring cellulose [19] and speleothems [20].

1 Study area

Eastern Monsoon China (EMC) is located to the east of 105°E , with the vast areas to the eastern part along the Greater Khingan Range-Kageyama-Alashan-Nyainqentanglha Mountains-Hengduan Mountains [21]. The topography is dominated by plain and mainly situated on the third terrace. The Eurasia is located to the north of EMC, and the vast Pacific Ocean faces the eastern side of EMC. Under the control of Siberian High, the strong cold air is characterized by frequent activities and less precipitation in winter. While in the summer, the Pacific warm air prevails here, and the rainfall is abundant [22]. Yearly-mean surface air temperature decreases from above 20°C in South China to about 0°C in Northeastern China (Figure 2(a)). Yearly-mean precipitation amount ranges from 200 to 2200 mm with a decreasing tendency of 1400 to 2000 mm in southeastern coastal areas, 800 to 1600 mm in the lower Yangtze region, 600 to 900 mm in South China and 200 to 800 mm in Northeastern China (Figure 2(b)) [23]. In the following discussion, the

EMC will be divided into three regions, Northeastern China, North China and Southern China in terms of the Chinese natural district region plot [24].

2 Data and method

Monthly composite precipitation samples collection has been carried out over the observation period years 2005 and 2006, at 17 CHNIP (Chinese Network of Isotopes in Precipitation) field stations [25]. There are total 17 stations located in EMC, among which eight stations are located in Southern China, six in North China and three in Northeastern China (Figure 2(c)).

Precipitation sampling method: in each filed station, a set composite of a Polyethylene bottle and a funnel was placed outside as a rain collector. A pingpong ball was put at the funnel to prevent evaporation. Snow samples were collected using a pail installed on the ground. After each snowfall event, snow samples melt at the room temperature. These two kinds of samples were transferred into a 50 mL polyethylene bottle as monthly samples and analyzed in the Environmental Isotopes Laboratory of Institute of Geographic Sciences and Natural Resources Research, Chinese Academy of Sciences. A Finnigan MAT253 mass spectrometer and the TC/EA method were used to carry out the isotopic measurements, and the results were expressed conventionally as δ -values, representing deviation in per mil (‰) from the isotopic composition of a specified standard (Vienna Standard Mean Ocean Water, V-SMOW), namely $\delta = 1000 \times [(R_{\text{sample}}/R_{\text{standard}}) - 1]$, where R refers to $^2\text{H}/^1\text{H}$ or $^{18}\text{O}/^{16}\text{O}$ ratios in both sample and standard. The measurement accuracy was consistently $\pm 1\text{‰}$ for δD and $\pm 0.3\text{‰}$ for $\delta^{18}\text{O}$ respectively.

Over the observation period, a total of 274 samples has been obtained at observation sites, 134 groups in the year 2005 and 140 groups in the year 2006. Routing meteorological variables, including wind, temperature, humidity,

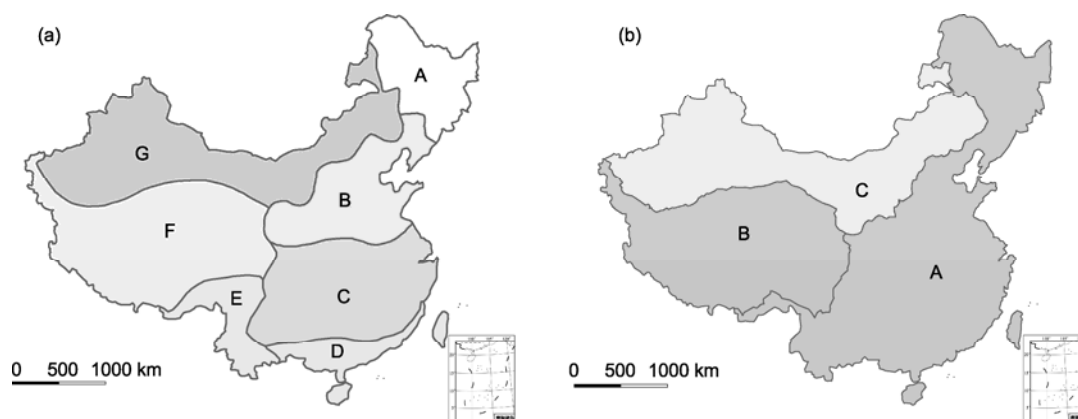


Figure 1 Chinese natural district region plots. (a) A, Northeastern area; B, North China; C, Central China; D, South China; E, Kangdian; F, Tibetan Plateau; G, Mengxin [24]; (b) A, Eastern Monsoon China; B, Tibetan Plateau; C, Arid Northwestern China [21].

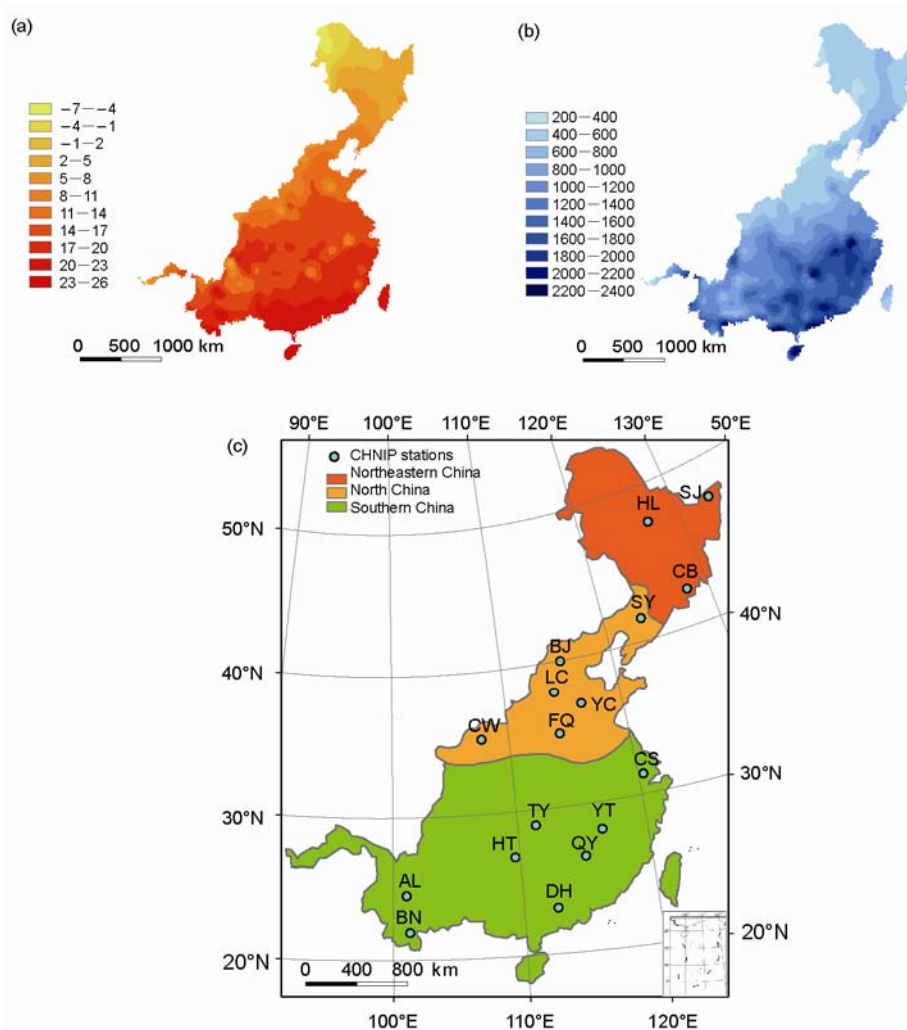


Figure 2 Distributions of yearly averaged temperature (a) and precipitation amount (1961–2000, 40 years averaged) (b); (c) locations of CHNIP stations in Eastern Monsoonal Region. SJ, Sanjiang; HL, Hailun; CB, Changbaishan; SY, Shenyang; BJ, Beijing; LC, Luancheng; YC, Yucheng; CW, Changwu; FQ, Fengqiu; CS, Changshu; TY, Taoyuan; QY, Qianyanzhou; YT, Yingtan; DH, Dinghushan; HT, Huitong; AL, Ailaoshan; BN, Xishuanbanna.

radiation, and precipitation amount, were routinely observed at each monitoring station, and the data set was compiled by the Synthesis Centre of Chinese Ecosystem Research Centre (CERN). The NCEP/NCAR reanalysis data sets from the NOAA-CIRES Climate Diagnostics Centre were employed at $2.5^{\circ} \times 2.5^{\circ}$ resolution to calculate water flux at the study area. All of the data sets were used at a monthly scale.

3 Results

3.1 LMWL of EMC

Based on the 274 groups of δD and $\delta^{18}O$ components in precipitation, a best-fit Local Meteoric Water Line (LMWL)

has been drawn through all the clusters ($\delta D = 7.46 \delta^{18}O + 0.90$, $R^2 = 0.94$), which provided an isotopic input function for local hydrological studies (Figure 3). Furthermore, the δD values varied between -208.05‰ – $+3.33\text{‰}$ and the $\delta^{18}O$ values ranged between -28.21‰ – $+0.38\text{‰}$. Amount-weighted δD and $\delta^{18}O$ values of precipitation were -50.77‰ and -6.91‰ , respectively, and among the three subregions, Southern China had the highest isotopic values ($\delta D = -44.68\text{‰}$, $\delta^{18}O = -6.25\text{‰}$); Northeastern Region had the lowest values ($\delta D = -99.21\text{‰}$, $\delta^{18}O = -12.78\text{‰}$); and North China's values were in the middle ($\delta D = -55.02\text{‰}$, $\delta^{18}O = -7.45\text{‰}$), which was also a reflection of the successively distillation of the heavy isotopes in the water vapor from the ocean to the inner continent, namely the continental effect.

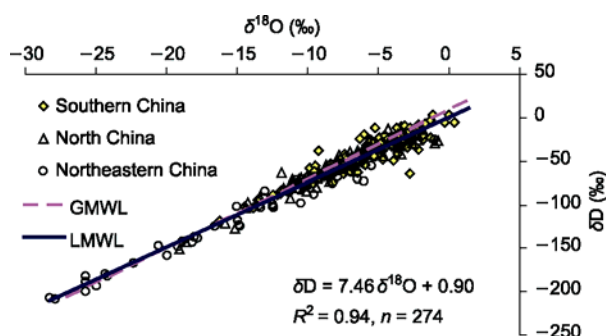


Figure 3 Local meteoric water line of Eastern Monsoon Region.

3.2 Temporal variations of $\delta^{18}\text{O}$ in precipitation

As there was a linear relationship between δD and $\delta^{18}\text{O}$ above, main discussions of characteristics will be focused on $\delta^{18}\text{O}$. Variation ranges of $\delta^{18}\text{O}$ in precipitation are reported in Table 1 along with the amount-weighted $\delta^{18}\text{O}$ values of precipitation. Among the three subregions, the largest $\delta^{18}\text{O}$ range was found in Northeastern China, and the smallest one was in coastal Southern China. The amount-weighted $\delta^{18}\text{O}$ in the year 2005 were all higher than that in 2006 over the whole study area. Moreover, time series of monthly $\delta^{18}\text{O}$ showed clear regional differences in both of the magnitude of the annual cycle and the response to the inter-annual variations in climate. At Southern China stations, precipitation became progressively depleted in $\delta^{18}\text{O}$ values during the summer monsoonal period (namely about May to August) and it was successively enriched in the winter monsoonal period. However, in Northeastern China this temporal variation was on the contrary, the isotopic composition of precipitation was enriched in $\delta^{18}\text{O}$ during the warmer months and depleted in the colder months (Figure 4). Colder temperature at higher latitude resulted in reductions in the total precipitable water in the atmosphere, leading to larger effective rainout of air masses [5]. Gibson [26] also have suggested that substantial seasonal patterns were typical, especially in cold regions, with winter precipitation generally strongly depleted and more variable in heavy-isotope content compared with that received during the summer season. Furthermore, seasonal changes typically produced shifts along the LMWL, which also accounted for the extended range of isotope compositions observed in monthly $\delta^{18}\text{O}$ values (Figure 3).

Table 1 $\delta^{18}\text{O}$ ranges in three subregions of Eastern Monsoon China

Region	$\delta^{18}\text{O}$ range (‰)	Amount-weighted $\delta^{18}\text{O}$ values of precipitation (‰)	
		2005	2006
Southern China	-16.2–0.38	-6.5	-5.94
North China	-19.07–-0.8	-8.46	-6.72
Northeastern China	-28.21–-0.99	-13.70	-11.66

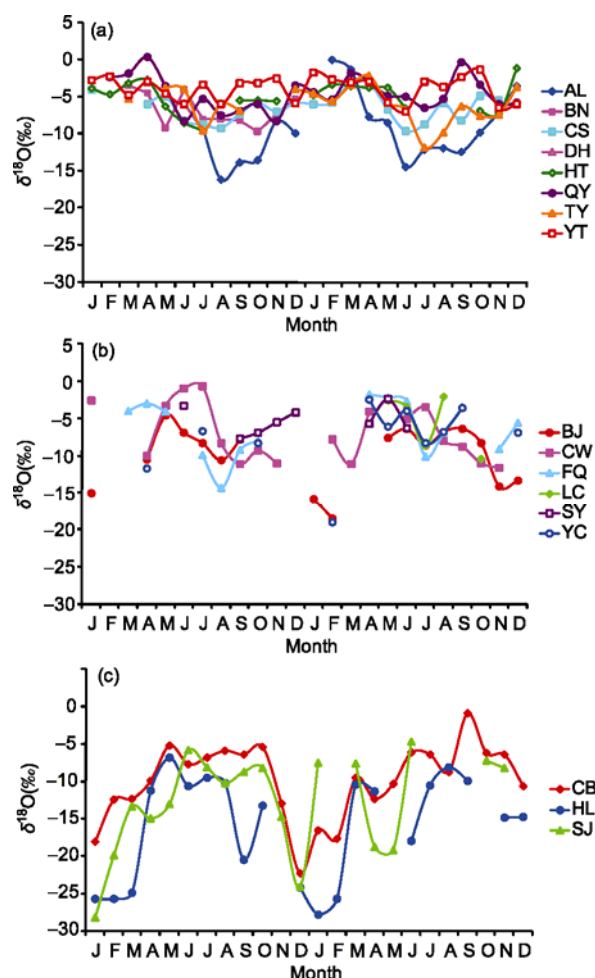


Figure 4 Temporal variations of $\delta^{18}\text{O}$ in EMC stations during 2005–2006. (a) Southern China; (b) North China; (c) Northeastern China. The legends are the same as in Figure 2.

3.3 Temperature and amount effect of $\delta^{18}\text{O}$ in precipitation

During the last five decades, abundant researches have proven that stable Oxygen and Hydrogen isotope components in precipitation were apparently affected by a number of factors including the specific evaporation conditions of the original moisture sources, rainout routes or transport patterns of the air masses from the ocean to the inland continents, and fractionation and condensation processes [27–35].

Table 2 Correlation coefficients between meteorological parameters and $\delta^{18}\text{O}$ in precipitation

Region	P	T_1	T_2	W_p	V_p	RH	R	S	W_s	W_d
EMC	0.181 ^{a)}	0.535 ^{a)}	0.522 ^{a)}	0.352 ^{a)}	0.111	0.014	0.063	0.037	-0.284 ^{a)}	-0.271 ^{a)}
SC	-0.182 ^{b)}	-0.199 ^{b)}	-0.244 ^{a)}	-0.248 ^{a)}	0.503 ^{a)}	-0.321 ^{a)}	-0.221 ^{b)}	0.031	-0.203 ^{b)}	0.112
NC	-0.015	0.362 ^{a)}	0.401 ^{a)}	0.290 ^{b)}	0.241 ^{b)}	0.589 ^{a)}	-0.024	0.577 ^{a)}	0.227	0.121
NEC	0.413 ^{a)}	0.644 ^{a)}	0.616 ^{a)}	0.504 ^{a)}	-0.344 ^{a)}	0.064	0.437 ^{a)}	0.283 ^{b)}	-0.294 ^{b)}	-0.207

EMC, Eastern Monsoon China; SC, Southern China; NC, North China; NEC, Northeastern China. P , precipitation amount (mm), T_1 , surface air temperature ($^{\circ}\text{C}$), T_2 , dew point temperature ($^{\circ}\text{C}$), W_p , water vapour pressure (hPa), V_p , air pressure (hPa), RH, relative humidity (%), R , total radiation (MJ/m^2), S , daylight hours (h), W_s , wind speed (m/s), W_d , wind direction; a) $P < 0.01$; b) $P < 0.05$.

Table 2 shows the corelationship between meteorological variables routinely observed at each field station and $\delta^{18}\text{O}$ in precipitation. Different regions have different dominant affecting factors. For instance, over the whole study area EMC, precipitation amount, temperature (both surface air temperature and dew point temperature), water vapor pressure and wind (wind speed and wind direction) were prominent meteorological variables controlling the $\delta^{18}\text{O}$ in precipitation, whereas, in the other three subregions, the dominant impact factors may change to others.

Among the meteorological factors, the two most important variables affecting the stable isotope ratios in precipitation are temperature and precipitation amount, which might be primarily ascribed to the temperature control effect through phase changing during the isotopic fractionation processes. On the other hand, strong convective phenomenon is the important factor restricting the isotopic composition variations across costal regions [29]. Over Southern China, which is nearest to the sea, the upper limited values of $\delta^{18}\text{O}$ in precipitation displayed a decreasing trend, and a slender amount effect was in concurrent ($\delta^{18}\text{O}$ (‰) = $-0.006P$ (mm) -5.16). However, the $\delta^{18}\text{O}$ values presented depleted as the surface air temperature rising. This phenomenon has confirmed the traditional concept that in the island or coastal regions, the amount effect may cover the temperature effect to some extent, or even, appearing a reverse temperature effect [36]. In North China and Northeastern China, as extending to the inner continent, temperature progressively replaced the precipitation amount and became the dominant control factor. Figure 5(b) and (c) show that there was not an amount effect at a year scale, however, if only the main summer rainfall period was taken into account, the amount effect could be expressed as $\delta^{18}\text{O}$ (‰) = $-0.02P$ (mm) -5.72 and $\delta^{18}\text{O}$ (‰) = $-0.02P$ (mm) -7.25 respectively [14].

3.4 Latitude and altitude effect of $\delta^{18}\text{O}$ in precipitation

The continental effect describes the progressive rainout and depletion of heavy isotopes ($\delta^{18}\text{O}$ and δD) from air masses as they traversing continental regions. Evaporation from the ocean is a fundamental source of global atmospheric moisture, which provides the precipitation input for continental

water cycling. Polar movement of tropical air results in a gradual rain-out and preferential loss of the heavier oxygen-18 during condensation. This process results in the depletion of $\delta^{18}\text{O}$ between tropical and temperate storm tracks, regardless of longitude [37–40]. The altitude effect describes the decreasing δ -values with increasing elevation, and is a variant of the temperature effect because temperatures typically decrease linearly with increasing altitude [41]. Moreover, locations and height of the groundwater recharge estimation is possible in virtue of the altitude effect of stable isotopes.

Correlation coefficients of $\delta^{18}\text{O}$ in precipitation vs. latitude and altitude are listed in Table 3. It showed that in Southern China and North China, main geographic factor that controlled the $\delta^{18}\text{O}$ in precipitation was altitude, and the quantitative relation was $-0.2\text{‰}/100$ m, namely, the $\delta^{18}\text{O}$ depleted 0.2‰ with the elevation increasing 100 m. This variation gradient was close to -0.28‰ per 100 m at an elevation of below 5000 m in mid- and low-latitude regions [42]. Altitude control factor changed to latitude in the more inner continental region of Northeastern China, and the relationship was -0.91‰ per 1° in latitude.

Table 3 Correlation coefficients of $\delta^{18}\text{O}$ in precipitation vs. latitude and altitude

Region	Correlation coefficients		Equation
	Latitude	Altitude	
EMC	-0.509 ^{a)}	-0.137 ^{b)}	$\delta^{18}\text{O} = -0.353\text{Lat} - 0.002\text{Alt} + 5.059$
SC	0.166	-0.457 ^{a)}	$\delta^{18}\text{O} = -0.002\text{Alt} - 4.983$
NC	-0.145	-0.276 ^{b)}	$\delta^{18}\text{O} = -0.002\text{Alt} - 6.327$
NEC	-0.336 ^{a)}	0.277 ^{b)}	$\delta^{18}\text{O} = -0.909\text{Lat} + 28.601$

a) $P < 0.01$; b) $P < 0.05$.

4 Discussion

4.1 Implications of the monsoon and rainfall belt movement

Seasonal variations in Asian monsoon primarily present as the occurrence of Eastern Asian monsoon. Generally, the

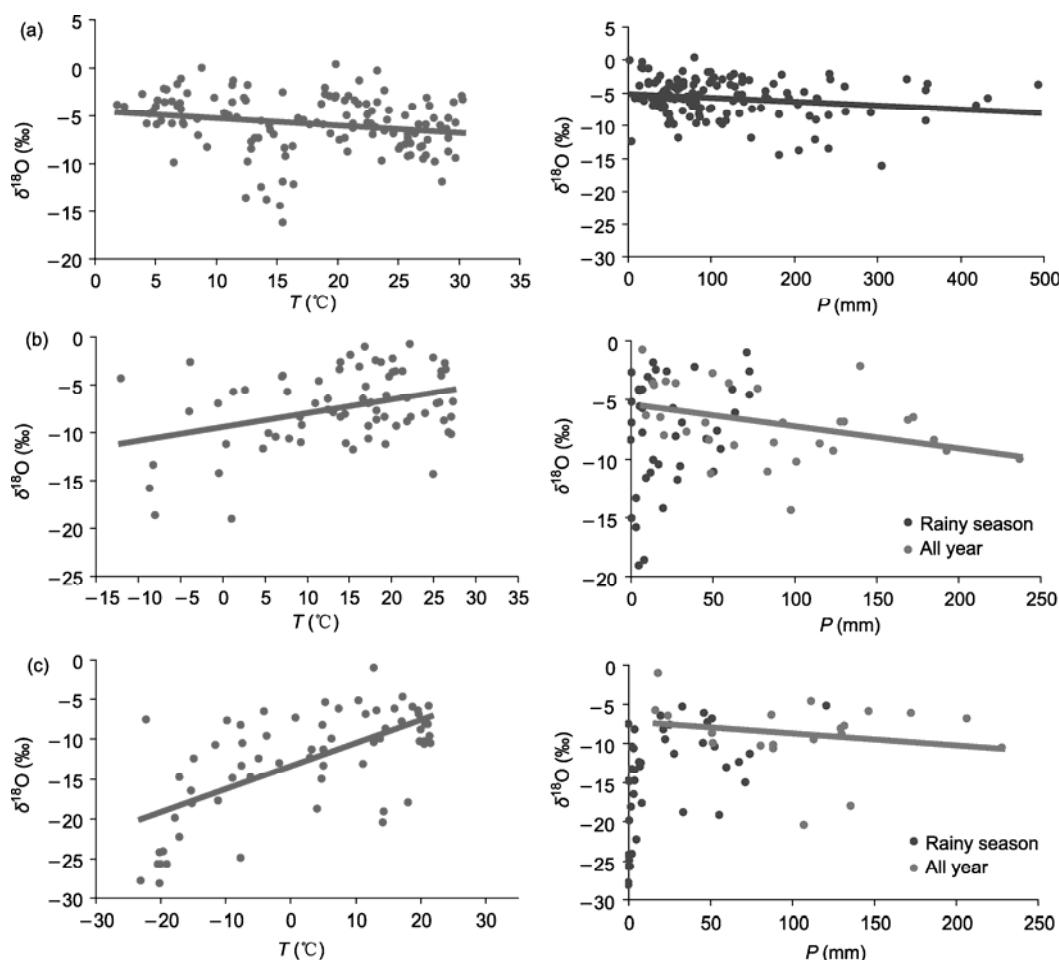


Figure 5 $\delta^{18}\text{O}$ O-T and $\delta^{18}\text{O}$ -P correlations. (a) Southern China; (b) North China; (c) Northeastern China.

Eastern Asian monsoon comes into being in mid-May, while Southern Asian monsoon forms in early-June, and the seasonal changes in the atmospheric circumfluence including rainfall in the monsoonal regions occurs during June [43–48]. Another obvious seasonal variation in Asian monsoon takes place during mid-September to October. At lower layers, it displays as the withdrawal of summer monsoon and onset of winter monsoon [49], which generally lasts until April or May of the next year [50]. At the same time, the movement of eastern Asian summer rainfall belt is also related to the advance and retreat of the Eastern Asian monsoon's forefront [51]. Climatologically, there are three obvious advance processes of rainfall belts locations over the Eastern Monsoon Region. Firstly, during April to early May, rainfall mainly occurs in South China, namely fore-flood season rainfall of South China. Secondly, from May to early-June, the rainfall belt is usually situated to the south of Yangtze River, while in mid-June, it swiftly switches northward, and the Plum rain season in Yangtze River and the Huaihe River Valleys starts. Thirdly, during mid- to late-July, the rainfall belt again jumps northward and reaches North China, which is the ending of the Plum rain

season in Yangtze River and the Huaihe River Valleys, and rainy season in North China and Northeastern China begins (Figure 6).

Investigations have found out that the ratio of $^{18}\text{O}/^{16}\text{O}$, or $^2\text{H}/^1\text{H}$, can be used to determine the origin of the atmospheric condensates. The gradual decline trend in $\delta^{18}\text{O}$ values during May to June over Southern China indicated the onset of the summer monsoon and the advent of rainy seasons. For instance, the $\delta^{18}\text{O}$ value of AL station was -7.73‰ in April, while it decreased to -8.47‰ in May and -14.48‰ in June, respectively. Through July to September, with the rainy seasons arriving, the $\delta^{18}\text{O}$ value remained at a relative low level (Figures 4 and 6). There was a similar phenomenon at TY and HT station (in the middle part of Southern China) and at CS and QY station (in the eastern part of Southern China). Whereas in North China, there was a time lag of about one month in the mutation of $\delta^{18}\text{O}$ values. This accorded with the rainfall belt arriving at North China about one month later than Southern China. Moreover, changes from depletion to enrichment in $\delta^{18}\text{O}$ in Southern China and the reverse changes in Northeastern China indicated the winter monsoon comes into being and

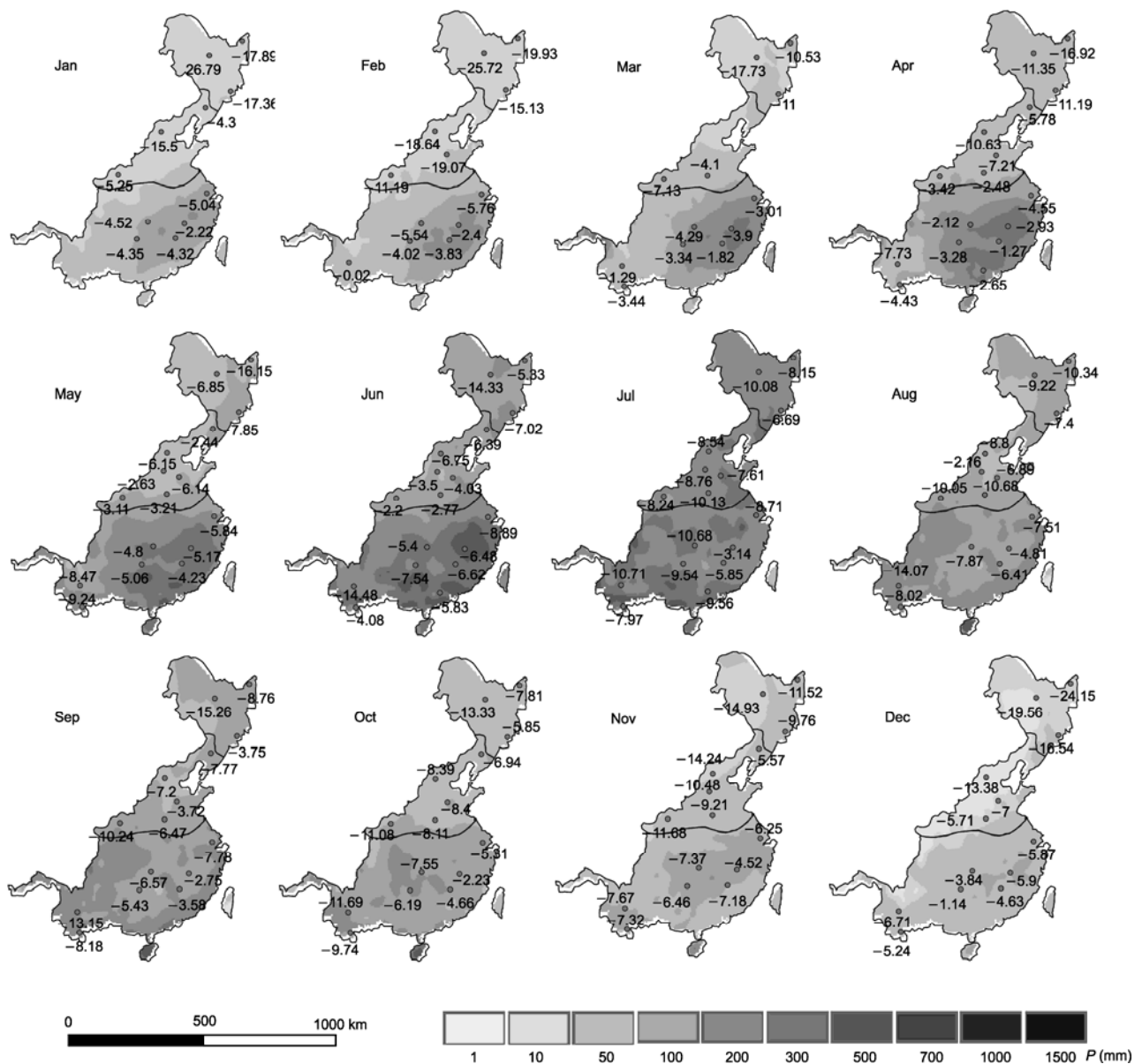


Figure 6 Spatial distributions of monthly precipitation amount and $\delta^{18}\text{O}$ values at CHNIP stations.

prevails. Furthermore, during June to July, when is the Plum rain period of Yangtze River and the Huaihe River Valleys, the $\delta^{18}\text{O}$ values of YT, QY, TY, HT and CS stations were keeping in a relative low level, somewhat it due in part to a successive equilibrium fractionation of the raindrop through the falling process under the condition of abundant water vapor supplement, high relative humidity, heavy cloud covers and relatively weak surface wind power. Generally, spatially variable moisture source and transport patterns have been identified for rainfall in the Asian summer monsoon by using the sea surface temperature, wind fields, low and high level air pressure anomalies, and precipitation patterns

[52]. Here, we found that the isotope in precipitation also had the implications of seasonal evolution and rainfall variability of the Asian summer monsoon.

4.2 Tracing the typhoons/severe tropical storms trajectories

The various isotope effects related to climatic processes may be described by progressive distillation of air masses. The isotope values of water are represented by the Rayleigh distillation equation ($\delta = \delta_0 \times f^{(\alpha-1)}$), where δ is the isotopic ratio, δ_0 is the initial isotopic ratio, f is the fraction of vapor remaining, and α is the fractionation factor for equilibrium

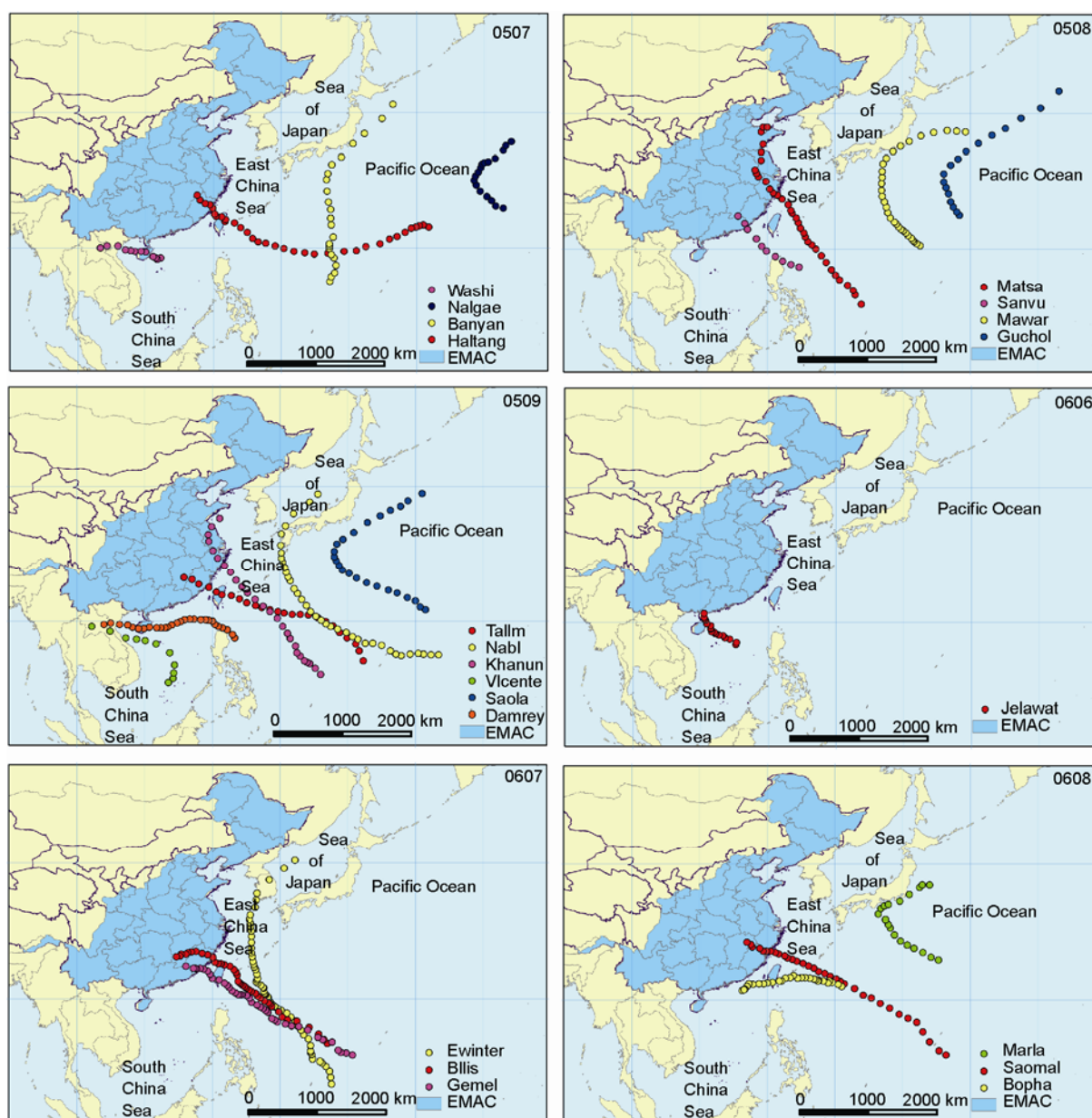


Figure 7 Tracks of typhoons or tropical storms occurred at west Pacific Ocean during the summer monsoonal period.

water-vapor exchange at the cloud temperature. The δ -value is not only related to the condensation temperature, but also related to remain vapor fraction [28]. During rainy seasons in Southern China, along the water vapor trajectory, variations of temperature at the cloud base was not remarkable. Therefore, δ could be considered controlled mainly by f through the journey of typhoons or severe tropical storms moving from ocean to inner continent. That is, the water vapor mass tends to be depleted of heavy isotope as the remaining precipitable water vapor decreased during the rainout process, namely, the δ -values tend to decreased.

The Western Pacific is a region where severe convection

weather such as typhoons or tropical storms frequently occurs. Trajectories during the summer monsoon period of the years 2005 to 2006 have been illustrated in Figure 7. The severe convection weather did brought effects on the rainfall over the southern and eastern coastal regions. According to the Rayleigh distillation concept, $\delta^{18}\text{O}$ component carried by the rear of typhoons might tend to be more negative than the frontal water vapor [53]. In July, 2005, there were four typhoons/severe tropical storms occurred round the study area. From spatial distributions of $\delta^{18}\text{O}$ contour lines, high $\delta^{18}\text{O}$ values appeared round Fujian Province, which was also the landing province of typhoon Haitang

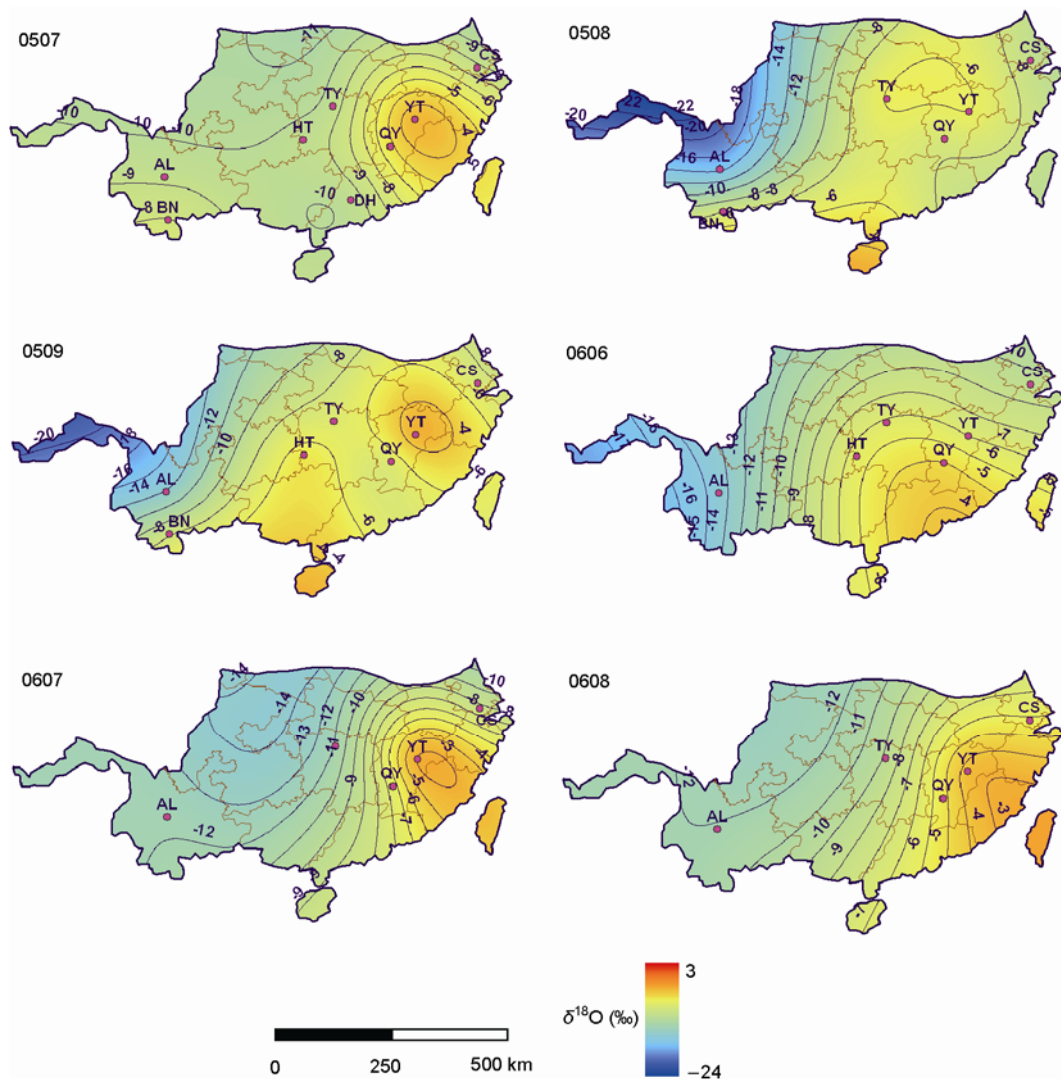


Figure 8 Contour lines of monthly $\delta^{18}\text{O}$ in precipitation over Southern China during the summer monsoonal period. The legends are the same as in Figure 2.

(No.0505). Furthermore, the direction of $\delta^{18}\text{O}$ contours line curve was also consisted with the water vapor transportation direction after typhoon Haitang landing (Figure 8). It proved that the isotopic information contained in precipitation has implications of severe convection weather. Again in August, 2005, times of typhoons/severe tropical storms occurrence were the same with that of July, 2005. Typhoon Matsa (No. 0509) landed at Zhejiang Province, and then influenced the regional rainfall at Shanghai, Jiangsu, Shandong, Tianjin and Liaoning Province. Regions included by the $\delta^{18}\text{O}$ contour line of -8‰ were in accordance with eastern coastal provinces which were exposed to Typhoon Matsa. In September, 2005, severe convection weather was quite active, and there were six in total. In eastern part, typhoon Talim (No. 0513) and Khanun (No. 0515) landed, and brought Fujian, Zhejiang, Jiangxi, and Anhui provinces rainfall of

high $\delta^{18}\text{O}$ component. The -6‰ contour line, which lied in Hainan, Guangxi and western Guangzhou, reflected their landing and movement into the inner continent of the typhoon. Talim, Khanun and Damrey have brought abundant moisture to provinces in eastern and southern China. As a whole, relative high $\delta^{18}\text{O}$ values in precipitation covered most of the southern area. In June, 2006, the Pacific Ocean surface was relatively calm, and there was only one typhoon, named Jelawat (No. 0602) landing on the boundary of Hainan, Guangdong and Guangxi. However, the spatial distribution of $\delta^{18}\text{O}$ did not reflect the landing place of Jelawat, but only the approximate movement direction of water vapor mass, which might possibly be due to short-lived duration of Jelawat (only three days). The moisture brought by it was limit. Therefore, as the monthly composite samples actually reflected the monthly mean condition, the trajectory

of Jelawat could not be identified. Similarly, the spatial distributions of $\delta^{18}\text{O}$ also had implications of the landing place and moisture movement from the ocean to the inner continental regions in July and August, 2006. The stable isotope signature of the precipitation directly links to the prevailing weather conditions during the rainfall event.

4.3 Proportions of moisture sources division

The division of proportions of multiple moisture sources is one of the breakthroughs obtained by application of isotopic method. This result may be difficult or impossible to be obtained using traditional meteorological and hydrological method. Former studies were mostly limited to the dichotomy of moisture sources, with the assumption that there were two moisture sources and ignoring other sources. As the stable oxygen-18 in precipitation had a good implication of the three main water vapor corridors during the summer monsoonal period over Southern China [9], here, isotopic fractionation models [54,55] were used to estimate proportions of multiple moisture sources in July, 2005. During the calculation, the water vapor flux data was utilized for the division of proportion of southwestern water vapor corridor (No. 1), South China Sea water vapor corridor (No. 2), southeastern water vapor corridor (No. 3) [56] and regional recycled water (No. 4) in each field station. Results (Table 4) were obtained by solving the equation groups:

$$\begin{cases} f_1 \times \delta^{18}\text{O}_1 + f_2 \times \delta^{18}\text{O}_2 + f_3 \times \delta^{18}\text{O}_3 + f_4 \times \delta^{18}\text{O}_4 = \delta^{18}\text{O}_{ek} \\ f_1 + f_2 + f_3 + f_4 = 1 \\ 0 \leq f_1, f_2, f_3, f_4 \leq 1, \end{cases} \quad (1)$$

where, f_{1-3} denoted the proportions of water vapor corridor No.1 to No.3; $\delta^{18}\text{O}_{1-3}$ were the $\delta^{18}\text{O}$ values of water vapor corridors No.1 to No.3 of either under equilibrium fractionation or kinetic fractionation; $\delta^{18}\text{O}_4$ was the $\delta^{18}\text{O}$ value of regional recycled water vapor proportion, and it was substituted by the $\delta^{18}\text{O}$ value of surface water $\delta^{18}\text{O}$ value observed simultaneously, and f_4 was its proportion; $\delta^{18}\text{O}_{ek}$ was the actual observation $\delta^{18}\text{O}$ value.

Furthermore, the basic forms of equilibrium and kinetic models of isotope are

$$\begin{cases} \delta^{18}\text{O}_e = \delta^{18}\text{O}_0 \times f^{(\alpha-1)} \\ \delta^{18}\text{O}_k = \delta^{18}\text{O}_0 + \Delta\varepsilon, \end{cases} \quad (2)$$

where $\delta^{18}\text{O}_0$ is the initial $\delta^{18}\text{O}$ value; $\delta^{18}\text{O}_e$ and $\delta^{18}\text{O}_k$ are the $\delta^{18}\text{O}$ values under equilibrium fractionation or kinetic fractionation respectively; α is fractionation coefficient at the temperature t ; $\Delta\varepsilon$ is an enrichment or depletion portion under a kinetic fractionation; f , the remaining water vapor flux, was calculated through the NCEP/NCAR reanalysis data at a monthly scale; unit side length water vapor transportation vector Q (kg/m·s) at all layers was calculated by

Table 4 Ratios of different water vapor origins at CHNIP stations during summer monsoon period of 2005

Station	f_1	f_2	f_3	f_4
AL	0–39%	18%–62%	0–64%	0–82%
BN	0–37%	0–98%	0–63%	0–92%
CS	25%–49%	0–75%	0–52%	0–63%
DH	42%–60%	0–58%	0–40%	0–48%
HT	0–44%	0–64%	0–39%	0–61%
QY	0–14%	0–34%	0–99%	0–86%
TY	40%–66%	0–60%	0–41%	0–34%

$$Q = \frac{1}{g} \int_P^{P_s} V q dP, \quad (3)$$

where V is wind speed vector at unit air column; q is absolute humidity; P_s , P are air pressure at lower boundary (ground air pressure) and upper boundary (200 hPa) respectively, and g is gravity acceleration.

As the unknown numbers were more than the equation numbers, the result f was actually the range of the value (Table 4). Moreover, certain values of f can be figured out if other related data was available.

5 Conclusions

The presented work analyzed the isotopic characteristics of precipitation over Eastern Monsoon China and assessed their physical controls.

Based on the 274 monthly samples throughout the years 2005 to 2006, LMWL has been established as $\delta\text{D} = 7.46 \delta^{18}\text{O} + 0.90$ ($R^2 = 0.94$), which reflected its particular local meteorological character. The δD and $\delta^{18}\text{O}$ values decreased from Southern China to North China to Northeastern China, which presented the heavy stable isotopes depleted as water vapor and subsequent precipitation moving inland.

The $\delta^{18}\text{O}$ values in the year 2006 over the whole study area were higher than those in the year 2005, and the variation of $\delta^{18}\text{O}$ values decreased from north to south. There was seasonal periodical variation of $\delta^{18}\text{O}$ in Southern China and Northeastern China. The $\delta^{18}\text{O}$ values depleted during summer monsoonal period and enriched during winter monsoonal period in Southern China while reversed in Northeastern China.

Dominating meteorological factors which affected the $\delta^{18}\text{O}$ values in precipitation varied in different regions. In coastal Southern China, the amount effect could be expressed as $\delta^{18}\text{O}(\text{‰}) = -0.006P(\text{mm}) - 5.16$, whereas in the inner continental regions of North China and Northeastern China, temperature effect gradually substituted the amount effect, and the amount effect only existed during main rainy season, their relationships were $\delta^{18}\text{O}(\text{‰}) = -0.02P(\text{mm}) - 5.72$ and $\delta^{18}\text{O}(\text{‰}) = -0.02P(\text{mm}) - 7.25$ respectively.

Altitude was the main geographic control on $\delta^{18}\text{O}$ in precipitation in Southern China and North China, and the quanti-

tative relationship was $-0.2\text{‰}/100\text{ m}$. However, in Northeastern China, the main control changed to latitude ($-0.91\text{‰}/\text{°}$).

Spatial distributions of $\delta^{18}\text{O}$ have implications for the onset and withdrawal of the monsoon, the movement of rainy belt of China and severe convection weather such as typhoons and severe tropical storms. Moreover, based on the isotopic fractionation models and water vapor flux data, proportions of water vapor sources (southwestern water vapor corridor, South China Sea water vapor corridor, southeastern water vapor corridor and regional recycled water vapor) have been estimated.

We thank the Synthesis Centre of Chinese Ecosystem Research Centre (CERN) and NOAA-CIRES (National Oceanic and Atmospheric Administration) for providing the meteorological data. Sincerely appreciation is given to the staff members of all the observatory field stations for collecting precipitation samples. Without their dedication this study would not have been possible. We are also grateful to Prof. Yang Jinrong and Yuan Jingjing for analysis of the water samples. Discussions with and encouragement from Prof. Ai Likun and Dr. Chen Feng from Institute of Atmospheric Physics, Chinese Academy of Sciences are invaluable. This work was supported by the National Natural Science Foundation of China (Grant Nos. 40830636 and 40671034), Foundation of Isotopes in Precipitation of Chinese Ecosystem Research Network.

- 1 Zhou S Z. Meteorology and Climatology (in Chinese). Beijing: Higher Education Press, 2005. 179
- 2 Ren M E. Chinese Physical Geography Compendium (in Chinese). Beijing: The Commercial Press, 1982. 47–56
- 3 Wei K Q, Lin R F. Influence of the monsoon on the isotope of precipitation in China (in Chinese). *Geochim*, 1994, 23: 33–40
- 4 Pang H X, He Y Q, Zhang Z L. Correlation between $\delta^{18}\text{O}$ in the monsoonal precipitation and some astronomy-atmosphere-ocean events (in Chinese). *J Glaciol Geocryol*, 2004, 26: 42–47
- 5 Welker J M. Isotopic ($\delta^{18}\text{O}$) characteristics of weekly precipitation collected across the USA: an initial analysis with application to water source studies. *Hydrol Process*, 2000, 14: 1449–1464
- 6 Ichiyonagi K, Yamanaka M. International variation of stable isotopes in precipitation at Bangkok in response of El Niño Southern Oscillation. *Hydrol Process*, 2005, 19: 3413–3423
- 7 Longinelli A, Anglesio E, Flora O, et al. Isotopic composition of precipitation in Northern Italy: reverse effect of anomalous climatic events. *J Hydrol*, 2006, 329: 471–476
- 8 He Y Q, Pang H X, Theakstone W H, et al. Isotopic variations in precipitation at Bangkok and their climatological significance. *Hydrol Process*, 2006, 20: 2873–2884
- 9 Liu J R, Song X F, Yuan G F, et al. Stable isotopes of summer monsoonal precipitation in southern China and the moisture sources evidence from $\delta^{18}\text{O}$ signature. *J Geogr Sci*, 2008, 18: 155–165
- 10 Zhang X P, Liu J M, Tian L D et al. Variations of $\delta^{18}\text{O}$ in precipitation along vapour transport paths over Asia (in Chinese). *Acta Geogr Sin*, 2004, 59: 699–708
- 11 Liu X C, Song X F, Xia J, et al. A study on oxygen isotope in precipitation of Dongtaigou basin in Chaobai River basin (in Chinese). *Geogr Res*, 24: 196–205
- 12 Liu X, Song X F, Xia J, et al. Characteristics of hydrogen and oxygen isotopes in preliminary analysis of vapor origin for precipitation at Chabagou catchment, Loess Plateau (in Chinese). *Resour Sci*, 2007, 29: 59–66
- 13 Sengupta S, Sarkar A. Stable isotope evidence of dual (Arabian Sea and Bay of Bengal) vapour sources in monsoonal precipitation over north India. *Earth Planet Sci Lett*, 2006, 250: 511–521
- 14 Yamanaka T, Tsujimura M, Oyunbaatar D, et al. Isotopic variation of precipitation over eastern Mongolia and its implication for the atmospheric water cycle. *J Hydrol*, 2007, 333: 21–34
- 15 Liu J R, Song X F, Sun X M, et al. Isotopic composition of precipitation over Arid Northwestern China and its implications for the water vapour origin. *J Geogr Sci*, 2009, 19: 164–174
- 16 Hoffmann G, Cuntz M, Jouzel J, et al. A systematic comparison between the IAEA/GNIP isotope network and the ECHAM 4 atmospheric general circulation model. In: Aggarwal P K, Gat J R, Froehlich K F O, eds. *Isotopes in the Water Cycle: Past, Present and Future of a Developing Science*. Vienna: International Atomic Energy Agency, 2005. 303–320
- 17 Hendricks M B, DePaolo D J, Cohen R C. Space and time variation of delta-oxygen 18 and delta-deuterium in precipitation: Can paleotemperature be estimated from ice cores? *Glob Biogeochem Cycles*, 2000, 14: 851–861
- 18 Dan H, Thomas W D E, Svante B. Climate and environment during the Younger Dryas (GS-1) as reflected by composite stable isotope records of lacustrine carbonates at Torreberga, southern Sweden. *J Quat Sci*, 1999, 14: 17–28
- 19 Leonel S L O S. Oxygen stable isotope of tree-ring cellulose: the next phase of understanding. *New Phytologist*, 2008, 1–10. doi: 10.1111/j.1469-8137.2008.02661.x
- 20 Ming T, Binggui C. Preliminary calibration of stalagmite oxygen isotopes from Eastern Monsoon China with Northern Hemisphere Temperatures, *PAGES News*, 2005, 13: 16–17
- 21 Huang B W. Draft on integrated physio-geographic regionalization of China (in Chinese). *Chin Sci Bull*, 1959, 18: 594–602
- 22 Song Y G, Yu S Y, Zhu C. Simulations of paleoclimate in the east China monsoon area since the last Glaciation (in Chinese). *Res Environ Yangtze Basin*, 1998, 7: 260–265
- 23 Zhao J, Chen C K. Geography of China (in Chinese). Beijing: Higher Education Press, 2005. 395–595
- 24 Luo K F. Draft on physio-geographic regionalization of China (in Chinese). *J Geogr Sci*, 1954, 20: 379–394
- 25 Song X F, Liu J R, Sun X M, et al. Establishment of Chinese Network of Isotopes in Precipitation (CHNIP) based on CERN (in Chinese). *Adv Earth Sci*, 2007, 22: 738–747
- 26 Gibson J J, Edwards T, Birks S J, et al. Progress in isotope tracer hydrology in Canada. *Hydrol Process*, 2005, 19: 303–327
- 27 Epstein S, Mayeda T. Variation of ^{18}O content of water from natural sources. *Geochim Cosmochim Acta*, 1953, 4: 213–224
- 28 Craig H. Isotopic variations in meteoric waters. *Science*, 1961, 133: 1702–1703
- 29 Dansgaard W. Stable isotopes in precipitation. *Tellus*, 1964, 16: 436–468
- 30 Craig H, Gordon L. Deuterium and oxygen-18 variations in the ocean and marine atmosphere. In: Tongiorgi E, ed. *Stable Isotopes in Oceanographic Studies and Palaeotemperatures*. Pisa: 1965. 9–130
- 31 Merlivat L, Jouzel J. Global climatic interpretation of the deuterium-oxygen-18 relationship for precipitation. *J Geophys Res*, 1979, 98: 5029–5033
- 32 Siegenthaler U, Oeschger H. Correlation of ^{18}O in precipitation with temperature and altitude. *Nature*, 1980, 285: 314–316
- 33 Rozanski K, Sonntag C, Münnich K O. Factors controlling stable isotope composition of modern European precipitation. *Tellus*, 1982, 34: 142–150
- 34 Johnsen S J, Dansgaard W, White J W C. The origin of Arctic precipitation under present and glacial conditions. *Tellus*, 1989, 41B: 452–468
- 35 Hoffmann G, Jouzel J, Masson V. Stable water isotopes in atmospheric general circulation models. *Hydrol. Process*, 2000, 14: 1385–1406
- 36 Yurtsever Y, Gat J R. Atmospheric waters. In: Gat J R, Gonfiantini R, eds. *Stable isotope hydrology: deuterium and oxygen-18 in the water cycle*. Vienna: International Atomic Energy Agency, 1981. 103–142
- 37 Gat J R, Matsui T. Atmospheric water balance in the Amazon Basin: an isotopic evapotranspiration model. *J Geophys Res*, 1991, 96: 179–183,188
- 38 Matthew S L, William P P. Use of correlation and stepwise regression to evaluate physical controls on the stable isotope values of Panamanian rain and surface waters. *J Hydrol*, 2006, 324: 115–140

- 39 Rindsberger M M, Magaritz I C, Gilad D. The relation between air mass trajectories and the water isotope composition of rain in the Mediterranean Sea area. *Geophys Res Lett*, 1983, 10: 43–46
- 40 Rozanski K, Araguás-Araguás L, Gonfiantini R. Isotopic patterns in modern global precipitation, *Geophysical Monograph*. In: Swart P K, Lohmann K L, McKenzie J, et al., eds. *Climate Change in Continental Isotopic Records*, American Geophysical Union, Washington DC, 1993, 1–36
- 41 Fricke H C, O'Neill J R. The correlation between $^{18}\text{O}/^{16}\text{O}$ ratios of meteoric water and surface temperature: its use in investigating terrestrial climate change over geologic time. *Earth Planet Sci Lett*, 1999, 170: 181–196
- 42 Poage M A, Chamberlain C P. Empirical relationships between elevation and the stable isotope composition of precipitation and surface water: considerations for studies of paleoelevation change. *Am J Sci*, 2001, 301: 1–15
- 43 Ye D Z, Tao S Y, Li M C. Abrupt Changes of atmospheric circumfluence during June and October (in Chinese). *Acta Meteorol Sin*, 1958: 249–263
- 44 Tao S, Chen L. A review of recent research on the East Asian Summer monsoon in China. *Monsoon Meteorology*. Oxford University Press, 1987. 60–92
- 45 Feng R Q, Wang A Y, Wu C S, et al. Climatological features of the establishment of South China Sea summer monsoon I—40-year mean (in Chinese). *J Trop Meteor*, 2001, 17: 345–354
- 46 Wang A Y, Feng R Q, Wu C S, et al. The inter-decade variation on climatic characteristics of the onset of South China Sea summer monsoon (in Chinese). *J Trop Meteor*, 2002, 18: 1–9
- 47 Liü J M, Zhang Q Y, Tao S Y, et al. Characteristics of the onset and advance of Chinese Asian monsoon (in Chinese). *Chinese Sci Bull*, 2006, 51: 332–338
- 48 Liü J M, Tao S Y, Zhang Q Y, et al. Processes of intraseasonal evolution of Asian summer monsoon under climatological mean condition (in Chinese). *Plateau Meteorol*, 2006b, 25: 814–823
- 49 Chen L X, Zhu Q G, Luo H B et al. *East Asian Monsoon* (in Chinese). Beijing: China Meteorological Press, 1991. 362
- 50 He J H, YU J J, Shen X Y, et al. Research on mechanism and variability of East Asian Monsoon (in Chinese). *J Trop Meteor*, 2004, 20: 450–458
- 51 Tao S Y. *Rainstorm of China* (in Chinese). Beijing: Science Press. 1980. 1–7
- 52 Lim Y K, Kim K Y, Lee H S. Temporal and spatial evolution of the Asian summer monsoon in the seasonal cycle of synoptic fields. *J Climate*, 2002, 15: 1580–1593
- 53 Shinji O, Yuki Y. Isotopic characteristics of typhonic rainwater: Typhoons No.13 (1993) and No.6 (1996). *Limnol*, 2000, 1: 143–149
- 54 Gat J R. Comments on the stable isotope method in regional groundwater investigations. *Water Resour Res*, 1971, 7: 980–993
- 55 Gonfiantini R. Environmental isotopes in lake studies. In: Fritz P, Fontes J C, eds. *Handbook of Environmental Isotope Geochemistry*, Vol. 2, the Terrestrial Environment, Amsterdam: Elsevier, 1996. 113–168
- 56 Tian H, Guo P W, Lu W S. Characteristics of vapor inflow corridors related to summer rainfall in China and impact factors (in Chinese). *J Trop Meteor*, 2004, 20: 401–408